JOURNAL OF THERMOPHYSICS AND HEAT TRANSFER
Vol. 8, No. 1, Jan.–March 1994

# Numerical Study of the Effects of Wall Catalysis on Shock Wave/Boundary-Layer Interaction

Adam Grumet,* John D. Anderson Jr.,† and Mark J. Lewis‡
*University of Maryland, College Park, Maryland 20742*

**This article presents a numerical study to investigate the effects of nonequilibrium chemistry, and in particular, wall catalysis on the separated flow region generated by an oblique shock wave impinging upon a flat plate boundary layer for a highly dissociated air flowfield. The results focus on the effects of the nonequilibrium chemistry upon the surface heat transfer and the separation zone size. Comparative results are given for chemically reacting (both noncatalytic and fully catalytic walls) and nonreacting flow cases. Furthermore, this comparison is extended over a wide range of freestream pressures (143–123,500 Pa) with a constant Reynolds number, $Re$ = 1793. A direct comparison of all three cases, at low pressures, reveals a minimal change in the peak heat transfer for the noncatalytic wall case as compared to the calorically perfect gas case. In contrast, the fully catalytic wall exerted a tremendous increase in the surface heat transfer. However, as the freestream pressure is increased, significant recombination occurs, so the increase in the peak heat transfer for the noncatalytic wall is more pronounced. Whereas for the fully catalytic wall, at higher pressures, the increase in peak heat transfer is somewhat diminished due to the chemical recombination upstream of the reattachment point.**

## Nomenclature

$C^+$ = characteristic
$c_i$ = mass fraction of species $i$
$D_{ij}$ = binary diffusion coefficient
$D_{im}$ = multicomponent diffusion coefficient
$d$ = molecular diameter
$e$ = internal energy
$IM$ = number of chemical species
$j_i$ = diffusion mass flux of species $i$
$k$ = coefficient of thermal conductivity
$k_b$ = backward reaction rate constant
$k_f$ = forward reaction rate constant
$M$ = Mach number
$M$ = molecular weight
$p$ = pressure
$q$ = heat flux
$R$ = gas constant
$Ru$ = universal gas constant
$T$ = temperature
$t$ = time
$U, E, F, J$ = vectorized variables for Navier-Stokes equations
$U_i$ = diffusion velocity
$u$ = parallel velocity component
$V$ = velocity
$v$ = normal velocity component
$X_i$ = mole fraction of species $i$
$[X_i]$ = concentration of species $i$
$\gamma$ = ratio of specific heats
$(\Delta H_f)_i^0$ = heat of formation at absolute zero
$(\varepsilon/k_l)$ = Leonard Jones parameter
$\theta_i$ = vibrational constant for species $i$
$\mu$ = viscosity coefficient
$\rho$ = density
$\tau$ = shear stress
$\phi$ = constant used in Wilke's rule
$\Omega$ = collision integral
$\omega_i$ = chemical source term for species $i$

Received Oct. 26, 1992; revision received March 10, 1993; accepted for publication March 26, 1993. 

*Graduate Research Assistant, Department of Aerospace Engineering. Student Member AIAA.
†Professor, Department of Aerospace Engineering. Fellow AIAA.
‡Assistant Professor, Department of Aerospace Engineering. Member AIAA.

## Introduction

AMONG the many different heat transfer problems encountered during hypersonic flight, one of the most significant will be the very large local peaks of heat transfer that can occur in the region where an oblique shock wave impinges upon a boundary layer. This interaction can occur in both external and internal flowfields. Examples of external interactions would be when the bow shock wave impinges upon the inside of the engine cowl lip or impinges upon the vehicle wing or any other body protrusion. An internal flowfield where the shock wave/boundary-layer interaction can occur is when shock waves reflect inside the combustion chamber, or when the shock wave emanating from the cowl lip reflects inside the diffuser.

Because of the importance of the shock wave/boundary-layer problem, and separated flow in general, there is an extensive volume of past work performed in this area over the past 45 yr. A sample of this volume is referenced in the following areas; analytical,[1] experimental,[2] and computational.[3–6] There has also been work that has included the effects of chemical reactions.[7,8]

The purpose of the present study is twofold: 1) to determine the effects of nonequilibrium chemistry, and in particular, wall catalysis on shock wave/boundary-layer interaction for hypersonic flow; and 2) to determine how varying the freestream pressure affects the influence of the catalytic wall on the flowfield. Consider the flow of air that passes through the normal portion of the detached shock, as seen in Fig. 1.

If the freestream Mach number is large (region 1), the temperature of the flow behind the shock (region 2) will be high enough for the air to chemically dissociate. The dissociated gas than cools as it expands around the forebody of the vehicle (region 3). If the expansion is rapid enough, there will not be enough time for recombination to occur. Therefore, the oxygen will probably be entirely dissociated and the nitrogen will also be dissociated to some degree. Inside the separated flow region (region 4), where the flow is recirculating, a large amount of chemical recombination may occur,

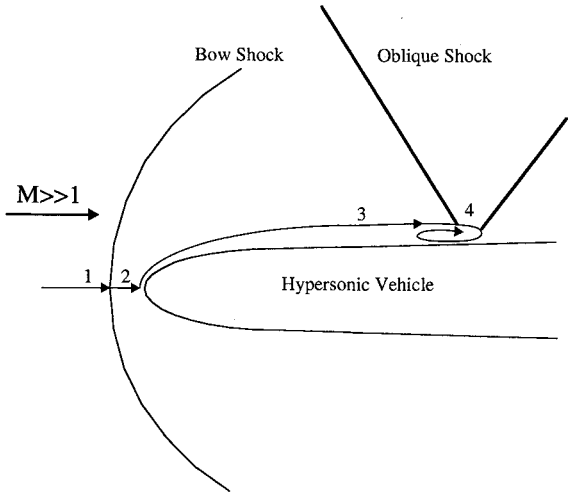


**Fig. 1 Schematic diagram of various reacting flowfields around the forebody of a hypersonic vehicle.**

thus releasing energy. This may, in turn, increase the surface heat transfer considerably. Furthermore, if the recombination is accelerated due to catalytic effects at the wall, the heat transfer may be even higher. Therefore, for all the cases considered in this investigation, the freestream air is considered to be in a highly dissociated state, thus emphasizing the above conditions.

## Computational Solution

### Governing Equations

For this study, the aforementioned physical problem was modeled by numerically solving the full two-dimensional, time-dependent, Navier-Stokes equations for nonequilibrium chemically reacting air. The Navier-Stokes equations in strongly conservative form is shown below:

$$\frac{\partial \boldsymbol{U}}{\partial t} + \frac{\partial \boldsymbol{E}}{\partial x} + \frac{\partial \boldsymbol{F}}{\partial y} = \boldsymbol{J} \tag{1}$$

Where the variables in vector form are

$$\boldsymbol{U} = \begin{bmatrix} \rho \\ \rho u \\ \rho v \\ \rho\left(e + \dfrac{V^2}{2}\right) \\ \rho c_i \end{bmatrix} \tag{2a}$$

$$\boldsymbol{E} = \begin{bmatrix} \rho u \\ \rho u^2 + p - \tau_{xx} \\ \rho uv - \tau_{xy} \\ \rho\left(e + \dfrac{V^2}{2}\right) u + pu - q_x - u\tau_{xx} - v\tau_{xy} \\ \rho c_i u - \rho D_{im} \dfrac{\partial c_i}{\partial x} + \rho c_i \sum_{j=1}^{IM} D_{jm} \dfrac{\partial c_j}{\partial x} \end{bmatrix} \tag{2b}$$

$$\boldsymbol{F} = \begin{bmatrix} \rho v \\ \rho uv - \tau_{yx} \\ \rho v^2 + p - \tau_{yy} \\ \rho\left(e + \dfrac{V^2}{2}\right) v + pv - q_y - u\tau_{yx} - v\tau_{yy} \\ \rho c_i v - \rho D_{im} \dfrac{\partial c_i}{\partial y} + \rho c_i \sum_{j=1}^{IM} D_{jm} \dfrac{\partial c_j}{\partial y} \end{bmatrix} \tag{2c}$$

$$\boldsymbol{J} = \begin{bmatrix} 0 \\ 0 \\ 0 \\ 0 \\ \dot{w}_i \end{bmatrix} \tag{2d}$$

In Eq. (2) the viscous stress tensors are

$$\tau_{xx} = \frac{2}{3}\mu\left(2\frac{\partial u}{\partial x} - \frac{\partial v}{\partial y}\right)$$

$$\tau_{yy} = \frac{2}{3}\mu\left(2\frac{\partial v}{\partial y} - \frac{\partial u}{\partial x}\right) \tag{3}$$

$$\tau_{xy} = \tau_{yx} = \mu\left(\frac{\partial u}{\partial y} + \frac{\partial v}{\partial x}\right)$$

and the energy transport terms are

$$q_x = k\frac{\partial T}{\partial x} + \sum_i \rho\left(D_{im}\frac{\partial c_i}{\partial x} - c_i \sum_{j=1}^{IM} D_{jm}\frac{\partial c_j}{\partial x}\right) h_i$$

$$q_y = k\frac{\partial T}{\partial y} + \sum_i \rho\left(D_{im}\frac{\partial c_i}{\partial y} - c_i \sum_{j=1}^{IM} D_{jm}\frac{\partial c_j}{\partial y}\right) h_i \tag{4}$$

Note that the energy transport equations for a chemically reacting gas, Eq. (4), consists not only of the energy transfer by thermal conduction, but also includes an additional term that accounts for mass diffusion. The mass diffusion term is important, especially in the vicinity of a catalytic wall.

### Chemical Rate Equations

The nonequilibrium chemistry was included in the problem by incorporating the modified Dunn-Kang chemical kinetics model. This model includes 5 species and 17 reactions.

$$\begin{aligned} O_2 + M &\rightleftharpoons 2O + M \\ N_2 + M &\rightleftharpoons 2N + M \\ NO + M &\rightleftharpoons N + O + M \\ O + NO &\rightleftharpoons N + O_2 \\ N_2 + O &\rightleftharpoons NO + N \end{aligned} \tag{5}$$

Where $M$ could be any one of the five possible collision partners. The reaction rate constants, $k_f$ and $k_b$, are determined from Arrhenius' equation:

$$k_f = A_f T^{Bf} e^{-(C_f/T)}$$

$$k_b = A_b T^{Bb} e^{-(C_b/T)} \tag{6}$$

The species mass fraction can then be obtained from the chemical concentration.

$$\rho c_i = [X_i] M_i \tag{7}$$

### Diffusion

For viscous, chemically reacting flow, mass diffusion becomes an important phenomena. That is, due to the random molecular motion, particles will diffuse when a species concentration gradient exists. The mass flux due to diffusion is approximated by a modified Fick's law[9]:

$$j_i \equiv \rho_i U_i = -\rho D_{im} \nabla c_i + \rho c_i \sum_{j=1}^{IM} D_{jm} \nabla c_j \tag{8}$$

Here, $U_i$ is the diffusion velocity of species $i$. Fick's law states that the gas will diffuse in the direction of decreasing species concentration. The last term on the right side of Eq. (8), as well as Eq. (4), assures that the summation of all the species mass fractions is unity. Without this term, mass will artificially be lost or gained.

The total velocity of the particle is the sum of the mixture velocity and the diffusion velocity:

$$V_i = V + U_i \tag{9}$$

If the concentration gradient is large enough, the diffusion velocity can be a dominant factor in the total velocity of a species in the flow.

The chemical diffusion is also a means of energy transport. As a given chemical species diffuses through the gas, it carries with it its species enthalpy. And just as in the case of the velocity, the energy flux due to diffusion can also be a dominant factor.

#### Transport Properties

The transport coefficients $\mu$ and $k$ are not simple functions of temperature, as they are for a calorically perfect gas. For a chemically reacting gas, they must be determined for each species and then combined to calculate the value for the gas mixture. This also applies to the chemical diffusivity $D$.

For the individual species, the viscosity and thermal conduction coefficients[10] in mks units are

$$\mu_i = 2.6693 \times 10^{-5} \frac{\sqrt{M_i T}}{d^2 \Omega_\mu}$$

$$k_i = 8.3221 \times 10^{-2} \frac{\sqrt{(T/M_i)}}{d^2 \Omega_k} \quad \text{atoms} \tag{10}$$

$$k_i = \mu_i \left(\tfrac{5}{2} c_{v_{\text{trans}}} + c_{v_{\text{rot}}} + c_{v_{\text{vib}}} + c_{v_{\text{elec}}}\right) \quad \text{molecules}$$

where the collision integrals are a function of temperature and the Leonard Jones parameters:

$$\Omega_\mu = \Omega_k = f\left(\frac{T}{\varepsilon/k_l}\right) \tag{11}$$

The diffusivity for a binary system (i.e., a two-component system) can be calculated in a similar fashion:

$$D_{ij} = 0.0188297 \frac{\sqrt{T^3 \, (1/M_i + 1/M_j)}}{p d_{ij}^2 \Omega_{d,ij}} \tag{12}$$

where

$$d_{ij} = \tfrac{1}{2}(d_i + d_j) \text{ avg diam}$$

$$\Omega_{d,ij} = f\left(\frac{T}{\varepsilon_{ij}/k_l}\right) \tag{13}$$

$$\frac{\varepsilon_{ij}}{k_l} = \sqrt{\frac{\varepsilon_i}{k_l} \frac{\varepsilon_j}{k_l}}$$

The transport properties for the gas mixture can then be evaluated from the individual components. For $\mu$ and $k$, Wilkes mixture rule is applicable. To calculate $D_{im}$, the following approximation was used:

$$D_{im} = \frac{1 - X_i}{\sum_{j=1}^{IM} \frac{X_j}{D_{ij}}} \tag{14}$$

#### Catalytic Walls

Just as there are wall boundary conditions for the velocity, such as the "no-slip" boundary condition, and for temperature, such as the adiabatic wall or a fixed temperature wall, there are also boundary conditions for the chemical mass fractions at the wall, which are determined by wall catalysis.

Because of the chemical properties of the wall itself, the rate at which reactions (dissociation or recombination) occur at the wall are affected. The exact mechanism of a catalytic wall is very complex, but Taylor[11] points out five mechanisms that determine the rate of reactions on the surface: 1) transport of reactants to the surface; 2) chemisorption of reactants on the surface; 3) chemical reactions between reactants adsorbed on the surface or between the reactant and an impinging molecule; 4) desorption of products from the surface; and 5) transport of products away from the surface.

Note the transport of the reactants and products to and from the surface is entailed in the diffusion mechanism.

This paper does not include any of the detailed mechanisms of wall catalysis; rather the simplifying assumption is made that wall catalysis can exist in varying degrees, and is a specified boundary condition.

The following terms are used to describe the various types of catalytic walls:

1) A noncatalytic wall is an extreme case in which no reactions occur at the wall, so the mass fraction gradient for all the species at the wall is zero

$$\left(\frac{\partial c_i}{\partial y}\right)_{y=0} = 0 \tag{15}$$

i.e., $(c_i)_{y=0} = (c_i)_{y=\Delta y}$.

2) A fully catalytic wall is the other extreme, where the chemical reactions at the wall are catalyzed at an infinite rate, so that the species mass fractions at the wall are at their local equilibrium value

$$(c_i)_{y=0} = (c_i)_{\text{equil}} \tag{16}$$

where $(c_i)_{\text{equil}} = f(p, T)$.

3) Finally, a partially catalytic wall falls between the above two extremes, where the chemical reactions at the wall are catalyzed at a finite rate. This can be simulated by either adjusting the reaction rate constants at the wall, or by setting the species mass fractions at the wall somewhere between their value above the wall and their equilibrium value. This study does not consider the partially catalytic wall case.

Consider a nonequilibrium dissociated flow that has expanded around the forebody of a hypersonic vehicle. The low temperature will promote recombination, thus releasing energy. If however, at the wall, the recombination is accelerated by wall catalysis, the additional energy release can be tremendous. Therefore, if a reasonable prediction of the wall heat transfer in a nonequilibrium flow is required, catalytic walls cannot be ignored.

#### Numerical Method

The governing equations are solved using MacCormack's explicit predictor-corrector technique, a well known time-dependent method useful for solving the combined hyperbolic-elliptic equations that are characteristic of the supersonic and subsonic flow regimes that occur in supersonic viscous flow problems. MacCormack's technique solves the first-order Taylor

series representation of the Navier-Stokes equations by using a predictor-corrector scheme to obtain second-order accuracy. MacCormack's predictor-corrector technique is explained in Refs. 10 and 12.

For the present investigation, the flowfield is solved on a two-dimensional rectangular grid which includes the plate surface and the freestream. A few pertinent details are discussed below.

#### Boundary Conditions

The treatment of the boundary conditions is not always straightforward, and frequently requires the most attention when solving the flowfield. The conditions that correspond to each of the boundaries is discussed below.

*Inflow Boundary*

For the inflow, the uniform freestream values are used. Recall from the introduction, that the freestream conditions have been selected to represent the relatively cool dissociated gas that has been expanded around an arbitrary blunt body traveling at hypersonic speeds.

Though important when requiring a practical shock wave/boundary-layer interaction calculation to include an inflow boundary layer profile, the thrust of this article was to generate comparative results for reacting/nonreacting and specifically catalytic/noncatalytic cases. Furthermore, this report represents ongoing research at the University of Maryland that studies the effects of nonequilibrium air chemistry on separated flows. The shock wave/boundary-layer interaction is simply a mechanism for producing such a flow. It is for these reasons that a more rigorous study, which would have included a boundary-layer inflow profile, was not performed.

*Outflow Boundary*

For the outflow, a linear extrapolation parallel to the freestream, is performed. Here $\boldsymbol{U}$ is calculated from the two upstream grid points:

$$\boldsymbol{U}_{X_{\max},Y} = 2\boldsymbol{U}_{X_{\max}-1,Y} - \boldsymbol{U}_{X_{\max}-2,Y} \tag{17}$$

*Upper Boundary*

For the flow adjacent to the freestream, i.e., the upward boundary condition, the conservative flux variables are extrapolated along the $C^+$ characteristics from the interior. This was done because of the skewness of the shock waves that would exit through this boundary.

An additional boundary condition must be supplied at the upper boundary in order to generate an oblique shock. The authors found that prescribing two thermodynamic variables (e.g., temperature and density) at the upper boundary, equal to the values corresponding to those behind an oblique shock of a given 1) shock angle, 2) freestream Mach number, and 3) freestream temperature and density is sufficient to generate the shock.

*Wall Boundary*

The final boundary condition that is applied is the wall. For viscous flow, a no-slip boundary condition is applied, where the flow velocity, both normal and parallel to the surface, is zero. Also, at the wall, the pressure gradient is assumed to be zero, i.e., $\partial p/\partial y = 0$:

$$p_{x,1} = \tfrac{1}{3}[4p_{x,2} - p_{x,3}] \quad \text{(second order)}: \quad 1 \le x \le x_{\max} \tag{18}$$

The temperature boundary conditions for a constant wall temperature (e.g., a cold wall)

$$T_{x,1} = T_{\text{wall}}: \quad 1 \le x \le x_{\max} \tag{19}$$

Recall from the introduction that additional boundary conditions must be supplied for chemically reacting flows with diffusion, namely, the catalytic wall boundary condition.

For a noncatalytic wall, a zero mass fraction gradient is imposed, i.e., $\partial c_i/\partial y = 0$:

$$(c_i)_{x,1} = \tfrac{1}{3}[4(c_i)_{x,2} - (c_i)_{x,3}] \quad \text{(second order)} \tag{20}$$

If the mass fraction gradients at the wall were calculated (for Fick's law) using a higher order extrapolation during the corrector step, the order of $\partial c_i/\partial y$ should be of the same order when determining the mass fraction at the wall.

For a fully catalytic wall, the mass fractions at the wall would be at the equilibrium value corresponding to the prescribed wall temperature, $T_{\text{wall}}$. If $T_{\text{wall}}$ is less than 2000 K (a "cold" wall), the mass fractions at the wall would be those of standard air (i.e., $c_{N_2} = 0.7778$, $c_{O_2} = 0.2222$). A realistic transatmospheric vehicle will probably require active surface cooling which would maintain a cold wall condition.

#### Artificial Viscosity

A common problem with time-dependent solutions of nonlinear problems is that small inaccuracies are introduced at the boundaries and in regions of sharp gradients. These inaccuracies can propagate as high-frequency disturbances (aliasing errors), which can cause the flow calculations to become unstable.[13] Therefore, it is required for this problem, to introduce explicitly an artificial viscosity term directly into MacCormack's technique.[14] This will dampen out the disturbances, and smooth out the numerical "overshoot" (dispersion errors) that are inherent in the second-order calculation of sharp gradients,[15] such as shock waves.

Because the magnitude of the numerical dissipation has a large effect on the quantitative results, especially in the separated region,[14] the values chosen for the dissipation constants (which are adjustable parameters) are kept reasonably small at 0.05.

## Results

A code was written to solve both the calorically perfect and chemically reacting (noncatalytic and fully catalytic) flowfields. The results given in this part of the article have three basic goals:

1) Display the qualitative and quantitative aspects of the aforementioned flowfields.

2) Compare, side by side, specific properties (e.g., heat transfer and surface shear stress) of these flowfields in order to assess the effects of chemical reactions and wall catalysis.

3) Show how increasing the freestream pressure affects the importance of nonequilibrium chemistry, in particular wall catalysis, on the shock wave/boundary-layer interaction flowfield.

#### Code Validation

For this article, successful comparisons for the calorically perfect case without an impinging shock were made with the analytical results obtained from the Van Driest boundary layer,[16] as well as from the reference temperature method for laminar flow over a flat plate.[10] Hence, confidence is obtained with the accuracy of the present Navier-Stokes code. Also, a direct comparison of surface heat transfer showed excellent agreement with the computational results obtained independently by Ballaro[8] for the calorically perfect shock wave/boundary-layer interaction.

In order to determine whether the computational solutions obtained are grid independent, a grid convergence check was performed for both calorically perfect and chemically reacting shock wave/boundary-layer interactions. Comparison of surface heat transfer results from three different grids: 1) 70 × 48, 2) 70 × 96, and 3) 70 × 192 for both reacting and nonreacting cases, revealed that the 70 × 96 grid was adequate.

## Calculated Results

*Low Pressure*

In this section, results are given that illustrate the effects of wall catalysis on a shock wave/boundary-layer interaction at a low freestream pressure. To do this, separate numerical solutions are shown for 1) calorically perfect case, 2) a chemically reacting, noncatalytic wall, and 3) a chemically reacting fully catalytic wall. Then a direct comparison of the surface heat transfer and shear stress between the three cases is made. Later in the article, results will be shown for a wide range of freestream pressures.

For each of the three cases, the parameters shown in Table 1 were constant.

For the chemically reacting cases, the following inflow species mass fractions were used, as shown in Table 2.

These conditions roughly correspond to a chemically frozen flow that has expanded around an arbitrary blunt forebody of a hypersonic vehicle traveling at Mach 25 at an altitude of 60 km.[7]

*Calorically Perfect Gas*

The first step towards modeling a shock/boundary-layer interaction with nonequilibrium chemistry and a fully catalytic wall, is to investigate the fluid dynamic effects of the interaction. This is done by neglecting the nonequilibrium chemical effects, thus assuming that the gas is calorically perfect. The results obtained from the calorically perfect case will serve as a bench mark from which we can compare the chemically reacting cases.

*Chemically Reacting Gas/Noncatalytic Wall*

For the chemically reacting/noncatalytic wall case, results are given that determine whether nonequilibrium chemistry plays a significant role in the shock wave/boundary-layer interaction.

Figure 2 is a pressure contour plot for the chemically reacting shock wave/boundary-layer interaction. The pressure contour plot clearly illustrates the incident and reattachment shock waves, as well as the shock wave induced by the separation zone. The recirculation zone is the low-pressure gradient region upstream of the reattachment shock.

Though not presented, the corresponding pressure contour plot for the calorically perfect gas case is virtually identical. This is because the magnitudes of the recombination for both oxygen and nitrogen are quite small. The percent differences between the maximum and minimum mass fractions inside the low freestream pressure flowfield for monatomic oxygen and nitrogen are 0.004 and 0.6%, respectively. Therefore, we can consider the flow to be essentially chemically frozen.

**Table 1 Freestream parameters**

| Parameter | Value |
|---|---|
| Freestream Mach number | 5.0 |
| Incident shock angle, deg | 30 |
| Wall temperature, K | 1087 |
| Freestream temperature, K | 1087 |
| Reynolds number, $Re_L$ | 1793 |
| Freestream pressure, Pa | 143 |
| Ratio of frozen specific heats | 1.48 |
| Gas constant, J/kg | 413.55 |
| Grid size | 70 × 96 |
| Plate length, m | 0.06 |

**Table 2 Inlet species mass fractions for chemically reacting cases**

| Species | Mass fraction |
|---|---|
| $O_2$ | 1.458 E-5 |
| O | 2.388 E-1 |
| $N_2$ | 5.500 E-1 |
| N | 2.111 E-1 |
| NO | 3.389 E-3 |

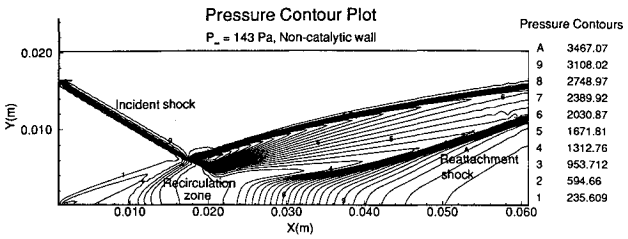


**Fig. 2 Pressure contour plot for a noncatalytic wall at $p_\infty$ = 143 Pa.**

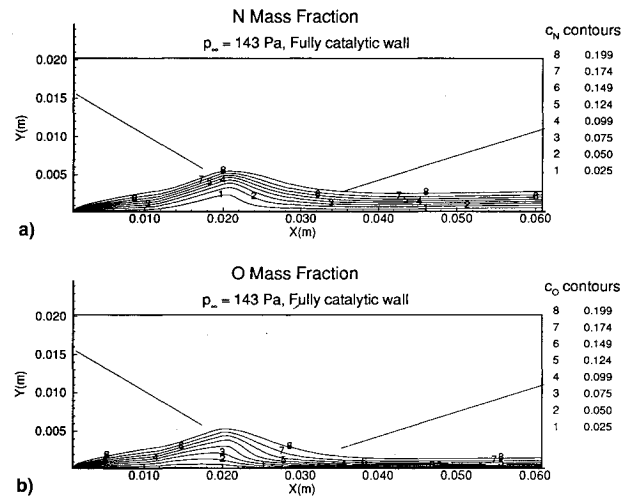


**Fig. 3 Species mass fraction contour plots for a fully catalytic wall at $p_\infty$ = 143 Pa: a) N and b) O.**

It is important to emphasize that both the qualitative and quantitative results are dependent upon flow conditions; wall and freestream temperatures, freestream pressures, and especially inlet species mass fractions; therefore, any conclusions that can be drawn from these results may not be applicable for all flow scenarios, as will be seen later on.

*Chemically Reacting Gas/Fully-Catalytic Wall*

In this section results are given for the chemically reacting fully catalytic wall case. These results will illustrate the effects of surface catalysis on the separated flow.

Figures 3a and 3b are the contour plots for the distribution of N and O species mass fractions throughout the flowfield. Included as a reference of the relative location of the separation zone, are lines signifying the incident and reattachment shock waves. The most apparent feature of these results is that the catalytic surface dominates the species mass fraction gradients. Although, because of the coarseness of the contours, it appears graphically that chemical reactions do not occur in the rest of the flowfield away from the wall, this is not true.

A main concern of this study is the coupled interaction between the separation zone and the catalytic surface. Considering the effects of the separation zone on the catalytic surface, we can see from the contour plots of O, and especially N, that the mass fraction gradient inside the separation zone is relatively mild. In the case of the monatomic nitrogen mass fraction, the large gradients encircle the separation zone so that the dramatic effects of the catalytic wall have been convected away from the surface in the separation region. The largest gradients of the species mass fractions occur behind the reattachment point, which further increases the heat transfer at the location where the maximum heat transfer is expected to occur.

*Comparisons of Results*

A direct comparison of the wall heat transfer between all three cases is shown in Fig. 4. Compared to the calorically perfect case, we can see that there is a negligible change in the heat transfer for the noncatalytic wall case. Again, it should be noted that the difference in the heat transfer is very dependent upon the values used for the inlet species mass fractions.

However, when we include the effects of wall catalysis, there is an increase of 135% for the surface heat transfer, as compared to the calorically perfect case. This was to be expected, considering the amount of energy that is being released at the surface due to instantaneous chemical recombination.

Please note that for the heat transfer plot shown in Fig. 4, as well as all other heat transfer plots presented in this article, the high heat transfer at the leading edge of the surface for the fully catalytic wall case is due to the sudden change in the chemical mass fractions between the inlet freestream values and the catalytic wall values over a distance of $\Delta y$. Hence, these values of heat transfer at the leading edge are not taken into consideration for comparative purposes.

A similar comparison is made for the surface shear stress, also shown in Fig. 4. One purpose of the shear stress plot is to effectively illustrate the size of the separation zone. The flow is reversed in the region where the surface shear stress is negative (below the dotted line). We can see from this figure that the nonequilibrium chemistry in the noncatalytic wall case has little effect on the size of the separation zone. This was expected due to the flow being essentially chemically frozen. The effects of wall catalysis on separation zone size is a bit more surprising. Considering the extent of chemical recombination at the surface, the changes in separation zone size are minimal. In fact, wall catalysis actually decreases the separation zone size slightly. As will be seen later on, chemical recombination inside the interior of the flowfield, as would occur for an increased freestream pressure, does increase separation zone size.

**Effects of Freestream Pressure**

For this study, a range of freestream pressures are used to represent both external and internal flowfields. The pressures used range from 143 to 123,500 Pa. For each case the Reynolds number was held constant by adjusting the flowfield length and height accordingly. This would isolate the effects of freestream pressures on chemical recombination.

The results shown earlier are for an external freestream pressure of 143 Pa, which corresponds to a dynamic pressure of 0.62 atm at a freestream Mach number equal to 25. The subsequent cases with higher freestream pressures do not correspond to different locations on the vehicle for similar flight parameters. Also, these cases do not correspond to different points along a similar flight trajectory. This article simply wants to include a demonstration of the effects of wall catalysis over a range of freestream pressure, while keeping the Reynolds number constant. By adjusting only the freestream pressure, the ability to keep the flight conditions along a single trajectory is lost.

A freestream pressure of 2860 Pa corresponds to a dynamic pressure equal to 0.5 atm and a freestream Mach number of 5. The internal freestream pressures of 47,500, 95,000, and 123,500 Pa all fall within a feasible range of combustion chamber pressures.

*Nitrogen*

The effects of increasing the freestream pressure are pronounced. For both the noncatalytic and fully catalytic wall cases, nitrogen recombination increases greatly with pressure. For a low freestream pressure, $p_\infty$ = 143 Pa, the maximum degree of $N_2$ recombination for the noncatalytic wall case is only 0.6%, which occurs inside the separation zone. However, for $p_\infty$ = 123,500 Pa, the maximum recombination is 87%. The effects that freestream pressure has on nitrogen species mass fractions in the flow are illustrated as flooded contours in Fig. 5, which is for a low freestream pressure and a fully catalytic wall. Because of the minimal degree of recombination, there is no plot for the low pressure noncatalytic wall. Figure 7, which is for a high freestream pressure, includes flooded nitrogen contours for both noncatalytic and fully catalytic wall cases. The relative location of recombination, which occurs inside and downstream of the separation zone, is apparent in Figs. 5 and 6 by overlapping pressure contours which highlight the incident shock, as well as the reflected and the shock caused by the front of the separation zone. As mentioned earlier, at lower pressures, recombination for the noncatalytic wall case is minimal. The fully catalytic wall does, of course, promote recombination along the plate surface, as

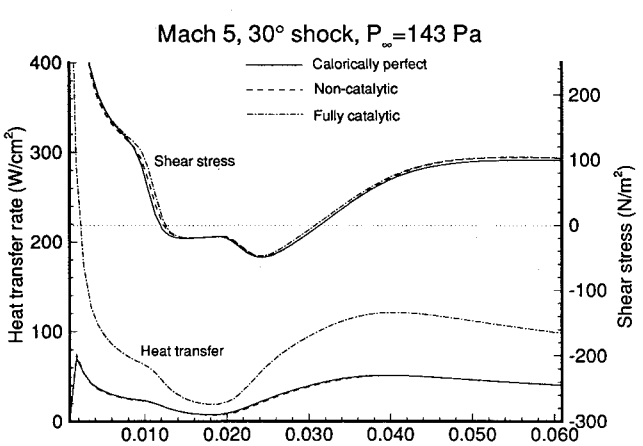


**Fig. 4 Comparative plots of surface heat transfer and shear stress at $p_\infty$ = 143 Pa.**

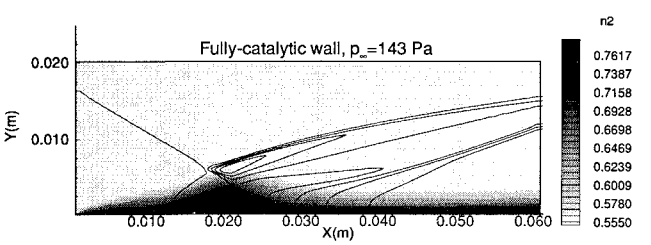


**Fig. 5 Nitrogen mass fraction flooded contour plots, with overlapping pressure contours at $p_\infty$ = 143 Pa: fully catalytic wall.**

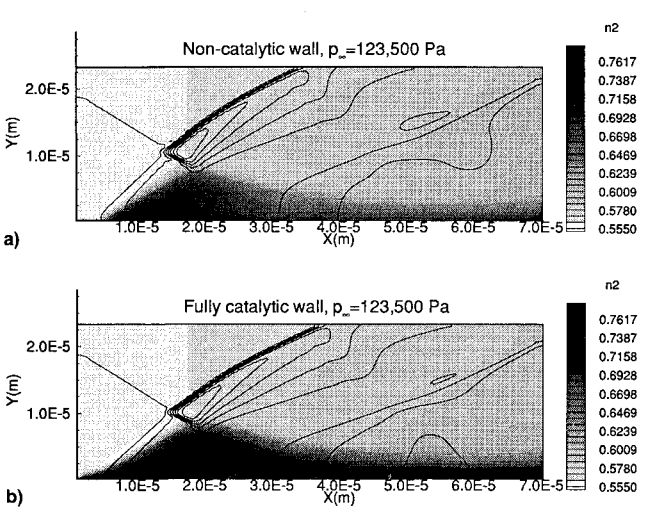


**Fig. 6 Nitrogen mass fraction flooded contour plots, with overlapping pressure contours at $p_\infty$ = 123,500 Pa: a) noncatalytic wall and b) fully catalytic wall.**

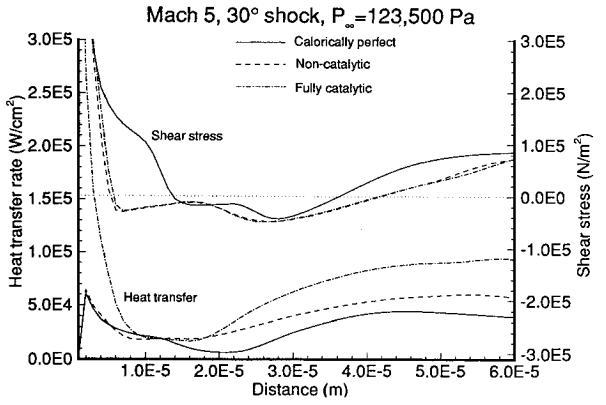


**Fig. 7 Comparative plots of surface heat transfer and shear stress at $p_\infty$ = 123,500 Pa.**

seen in Fig. 5. The high $N_2$ concentrations produced along the surface readily diffuse into the recirculation region, thus accounting for the relatively high concentrations in this region.

At higher pressures, significant recombination occurs throughout the flowfield for both fully catalytic and noncatalytic walls, especially inside the separation zone, as seen in Fig. 6. Because of the recombination due to the higher freestream pressure, the effects of wall catalysis are less significant.

Nitrogen recombination, which is most pronounced at higher pressures, greatly increases the temperature throughout the flowfield. For a freestream pressure of 123,500 Pa, there is a significant increase in the maximum temperature in a chemically reacting flowfield as compared to a nonreacting (calorically perfect) flowfield. The maximum temperature that occurs in the calorically perfect gas flowfield is 4653 K, whereas for the noncatalytic and fully catalytic wall cases, the maximum temperatures that occur are 5765 and 5831 K, respectively.

*Oxygen*

Because of the high flowfield temperatures, the oxygen, which is mainly all atomic, is hardly affected. Even at high pressures, only 7% maximum recombination occurs, therefore, the effects due to oxygen recombination for the noncatalytic wall cases are negligible. However, for the fully catalytic wall cases, oxygen recombination has a significant effect, especially near the wall. Furthermore, the oxygen recombination is relatively independent of freestream pressure.

*Surface Heat Transfer*

Results shown earlier in this article demonstrated the effects of nonequilibrium chemistry for a low freestream pressure was only important when coupled with wall catalysis. The percent increase in surface heat transfer, as compared to the calorically perfect gas case, was negligible for a noncatalytic wall. But, for a fully catalytic wall, the surface heat transfer increased drastically. However, that was for a low freestream pressure. We have seen that increasing pressure increases nitrogen recombination. So it is reasonable to expect that the additional energy release would increase the heat transfer at the surface. Let us now look at how increasing the freestream pressure affects the importance of nonequilibrium chemistry on surface heat transfer.

Figure 7 includes a plot of surface heat transfer for a calorically perfect gas, noncatalytic, and fully catalytic wall cases for a freestream pressure of 123,500 Pa. As expected, there is a significant increase in the heat transfer for the noncatalytic wall case. While there is still an increase in heat transfer for the fully catalytic wall case (as compared to the calorically perfect case), interestingly enough, the increase is not as large as for when the freestream pressure is lower. A possible reason for this is, at higher pressures, more recombination occurs upstream of the location of maximum heat transfer. Therefore, there is less chemical recombination due to wall catalysis at the point of maximum heat transfer, thus less energy release. The smaller increase in heat transfer for a catalytic wall coupled with the fact that there is a substantial increase in heat transfer for the noncatalytic wall, further downplays the importance of wall catalysis at higher pressures.

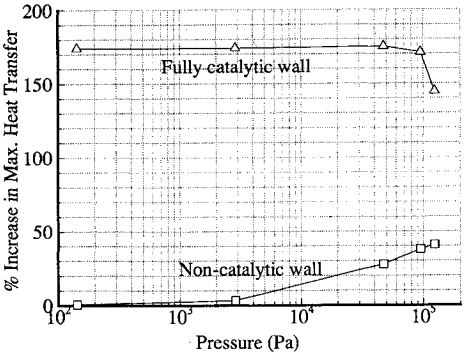


**Fig. 8 Percent increase in maximum heat transfer (relative to nonreacting case) vs freestream pressure.**

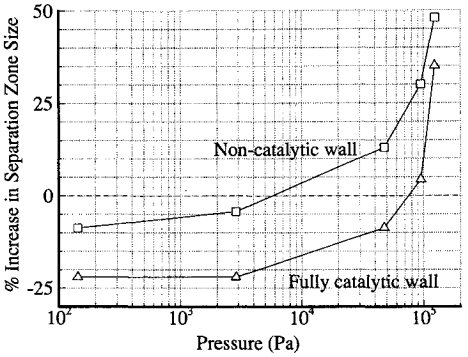


**Fig. 9 Percent increase in separation zone size (relative to nonreacting case) vs freestream pressure.**

Due to space limitations, the heat transfer plots for each freestream pressure case will not be presented. However, Fig. 8 is a plot of the percent increase of the maximum heat transfer (neglecting the leading edge) as compared to the calorically perfect gas case vs pressure, for both noncatalytic and fully catalytic wall cases. Clearly, we see how the noncatalytic wall heat transfer increase grows for increasing pressure, whereas the fully catalytic wall heat transfer increase begins to shrink at higher pressures. This plot further illustrates the growing importance of nonequilibrium chemistry and the decreasing importance of wall catalysis at higher freestream pressures.

*Separation Zone Size*

Recall that effective quantitative measures of separation zone size are skin friction plots. Figures 4 and 7 include comparative plots of the surface shear stress for $p_\infty$ = 143 and 123,500 Pa, respectively. Interestingly enough, there is little similarity between the two plots. At low pressure, the separation zone size is virtually the same for both reacting and nonreacting cases. Whereas for the high-pressure case, the calorically perfect gas case has the smallest separation zone size. For the entire pressure range, the noncatalytic wall has a slightly larger separation zone size than its fully catalytic counterpart. Figure 9 plots the percent change (compared to the calorically perfect gas case) of separation zone size versus pressure for both catalytic and noncatalytic wall cases.

## Conclusions

The purpose of this study is to determine the effects of nonequilibrium chemistry on the shock wave/boundary-layer interaction. Emphasis is placed on the importance of wall

catalysis and varying freestream pressure (thus simulating both external and internal flowfields), especially with regard to the surface heat transfer. The following conclusions can be drawn concerning the cases examined.

**Low Pressures**

1) Wall catalysis significantly increased the surface heat transfer and must be accounted for when designing a hypersonic vehicle.

2) The degree of chemical reaction, as demonstrated in the non-catalytic wall case, is very small. Therefore the flow is essentially chemically frozen for the case considered here.

Therefore, the effects of the nonequilibrium chemical reacting flow on the shock/wave boundary-layer interaction depends critically on the catalysis of the wall.

**Varying Pressures**

1) As freestream pressure increases, the degree of chemical reaction becomes more important. Especially for internal flows, where the pressure is of the order of magnitude of about 1 atm, the flow is no longer chemically frozen, even for the noncatalytic wall.

2) The importance of wall catalysis diminishes as the pressure increases. This is because a large percentage of the chemical recombination at the surface occurs due to the high flowfield pressures, and this recombination would have occurred regardless of wall catalysis. Also, much of the chemical recombination occurs upstream of the shock impingement point. So that the energy release, due to the presence of a catalytic wall, that occurs at the location of maximum heat transfer is reduced.

## Acknowledgments

This work was supported in part by AFOSR Grant 88.0101 with James Wilson and Len Sakell as grant monitors, and by NASA Ames Grant NAG-2-529 with George S. Deiwert as grant monitor. This project was in part completed through the use of a CRAY Y-MP and a CRAY X-MP which were graciously provided by NASA Langley Research Center and the Jet Propulsion Laboratory, respectively.

## References

[1]Goldstein, S., "On Laminar Boundary-Layer Flow Near a Point of Separation," *The Quarterly Journal of Mechanics and Applied Mathematics*, Vol. 1, Pt. 1, 1948, pp. 43–69.

[2]Bogdonoff, S. M., and Kepler, E. C., "Separation of a Supersonic Turbulent Boundary Layer," Princeton Univ., Dept. of Aerospace Engineering Rept. 249, Princeton, NJ, Jan. 1954.

[3]Issa, R. J., and Lockwood, F. C., "On the Prediction of Two Dimensional Supersonic Viscous Interaction Near Walls," *AIAA Journal*, Vol. 15, No. 2, 1977, pp. 182–188.

[4]Hodge, B. K., "Prediction of Hypersonic Laminar Boundary-Layer/Shock-Wave Interactions," *AIAA Journal*, Vol. 15, No. 7, 1977, pp. 903, 904.

[5]Horstman, C. C., "Prediction of Hypersonic Shock-Wave/Turbulent Boundary-Layer Interaction Flow," AIAA Paper 87-1367, June 1987.

[6]Payne, J. L., "The Effects of Nonequilibrium Chemical Reactions on Hypersonic Separated Flows in Air: Inviscid Flow Simulations," M.S. Thesis, Univ. of Maryland, College Park, MD, 1989.

[7]Ballaro, C. A., and Anderson, J. D., Jr., "Shock Strength Effects on Separated Flows in Non-Equilibrium Chemical Reacting Air Shock Wave/Boundary Layer Interaction," AIAA Paper 91-0250, Jan. 1991.

[8]Grumet, A. A., Anderson, J. D., Jr., and Lewis, M. J., "A Numerical Study of Shock Wave/Boundary Layer Interaction in Nonequilibrium Chemically Reacting Air: The Effects of Catalytic Walls," AIAA Paper 91-0245, Jan. 1991.

[9]Coffe, T. P., and Heimerl, J. M., "Transport Algorithms for Premixed, Laminar Steady State Flames," *Combustion and Flame*, Vol. 43, No. 3, 1981, pp. 273–289.

[10]Anderson, J. D., Jr., *Hypersonic and High Temperature Gas Dynamics*, McGraw-Hill, New York, 1989.

[11]Taylor, H. S., "Combustion Processes," *High Speed Aerodynamics and Jet Propulsion Series*, edited by B. Lewis, Vol. II, Princeton Univ. Press, Princeton, NJ, 1956.

[12]Grumet, A. A., "A Numerical Study of Shock Wave/Boundary Layer Interaction for Nonequilibrium Chemically Reacting Air: The Effects of Catalytic Walls," M.S. Thesis, Univ. of Maryland, College Park, MD, 1990.

[13]Anderson, J. D., *Modern Compressible Flow with Historical Perspective*, McGraw-Hill, New York, 1982.

[14]Kuruvila, G., and Anderson, J. D., Jr., "A Study of the Effects of Numerical Dissipation on the Calculations of Supersonic Separated Flows," AIAA Paper 85-0301, Jan. 1985.

[15]Anderson, D. A., Tannehill, J. C., and Pletcher, R. H., *Computational Fluid Mechanics and Heat Transfer*, Hemisphere, New York, 1984.

[16]Van Driest, E. R., "Investigations of Laminar Boundary Layer in Compressible Fluids Using the Crocco Method," NACA, TN 2597, Jan. 1952.